

Nonlinear waves in a multilayer system

Ilya B. Simanovskii^{a,b,*}, Antonio Viviani^c, Frank Dubois^d, Jean-Claude Legros^d

^a Department of Mathematics, Technion – Israel Institute of Technology, 3200 Haifa, Israel

^b Minerva Center for Nonlinear Physics of Complex Systems, Technion – Israel, Institute of Technology, 32000 Haifa, Israel

^c Seconda Università di Napoli (SUN), Dipartimento di Ingegneria Aerospaziale e Meccanica (DIAM), via Roma 29, 81031 Aversa, Italy

^d Université Libre de Bruxelles, service de chimie physique EP, CP165-62, 50, avenue F.D. Roosevelt, B-1050, Brussels, Belgium

Received 6 February 2009; accepted after revision 3 March 2009

Available online 3 April 2009

Presented by Jean-Baptiste Leblond

Abstract

The joint action of buoyant and thermocapillary mechanisms of instability in a multilayer system, is investigated. The nonlinear convective regimes are studied by the finite difference method. The periodic boundary conditions on the lateral boundaries, are considered. It is found that the competition of both mechanisms of instability may lead to the appearance of a buoyant–thermocapillary traveling wave and a modulated traveling wave. *To cite this article: I.B. Simanovskii et al., C. R. Mecanique 337 (2009).*

© 2009 Académie des sciences. Published by Elsevier Masson SAS. All rights reserved.

Keywords: Interfacial convection; Multilayer system; Finite difference method

1. Introduction

Convective phenomena in fluid systems with an interface have been a subject of an extensive investigation (for a review, see [1,2]). The description of the interfacial convection is based on different models. The simplest, “one-layer” model, considers the air/liquid interface as a “free surface”. In reality, “the free surface” is a simplified description of an interface between a liquid and a gas. When the “one-layer” approach is applied, the full problem for the liquid motion and for the heat/mass transfer is formulated *only* in the liquid phase, whereas the influence of the gas phase is described in a phenomenological way by means of the Biot number.

The one-layer approach is insufficient for the description of many phenomena caused by processes in fluids on both sides of the interface [2]. These phenomena cannot be understood without an analysis of the interfacial hydrodynamic and thermal interaction between both fluids. The more exact approach is the “two-layer approach” when equations and boundary conditions are written on both sides of the interface. This approach is used in the present Note.

There are two basic physical phenomena that produce convective instability in systems with an interface: buoyancy and thermocapillary effect. When heating is from below, the buoyancy instability generates the Rayleigh–Bénard

* Corresponding author.

E-mail address: yuri11@inter.net.il (I.B. Simanovskii).

convection [3], while the thermocapillary effect is the origin of the Marangoni–Bénard convection [4,1]. The case where both effects act simultaneously, is the most typical.

One of the interesting phenomena caused by the joint action of buoyancy and thermocapillary effect is the appearance of the oscillatory instability of the mechanical equilibrium by heating from below. This phenomenon was first discovered in the case of a two-layer system [5,1,6]. A similar phenomenon under the joint action of both mechanisms of instability in the multilayer system with free or rigid heat-insulated lateral boundaries, has been studied in [7]. Only regimes of standing waves have been found in [7].

In the present Note, we investigate the joint action of buoyant and thermocapillary mechanisms of instability in multilayer system air–ethylene glycol–fluorinert FC75 with periodic boundary conditions on lateral boundaries. It is found that the competition of both mechanisms of instability may lead to the development of nonlinear buoyant–thermocapillary traveling wave and modulated traveling wave.

2. General equations and boundary conditions

Let the space between two rigid horizontal plates be filled by three immiscible viscous fluids with different physical properties (see Fig. 1). The equilibrium thicknesses of the layers are a_m , $m = 1, 2, 3$. The m th fluid has density ρ_m , kinematic viscosity ν_m , dynamic viscosity $\eta_m = \rho_m \nu_m$, thermal diffusivity χ_m , heat conductivity κ_m and heat expansion coefficient β_m . The surface tension coefficients on the upper and lower interfaces, σ and σ_* , are linear functions of temperature T : $\sigma = \sigma_0 - \alpha T$, $\sigma_* = \sigma_{*0} - \alpha_* T$. The acceleration due to gravity is g . The horizontal plates are kept at different constant temperatures. The system is heated from below, and the overall temperature drop is θ .

We define

$$\rho = \frac{\rho_1}{\rho_2}, \quad \nu = \frac{\nu_1}{\nu_2}, \quad \eta = \frac{\eta_1}{\eta_2} = \rho\nu, \quad \chi = \frac{\chi_1}{\chi_2}, \quad \kappa = \frac{\kappa_1}{\kappa_2}, \quad \beta = \frac{\beta_1}{\beta_2}, \quad a = \frac{a_2}{a_1}$$

$$\rho_* = \frac{\rho_1}{\rho_3}, \quad \nu_* = \frac{\nu_1}{\nu_3}, \quad \eta_* = \frac{\eta_1}{\eta_3} = \rho_*\nu_*, \quad \chi_* = \frac{\chi_1}{\chi_3}, \quad \kappa_* = \frac{\kappa_1}{\kappa_3}, \quad \beta_* = \frac{\beta_1}{\beta_3}, \quad a_* = \frac{a_3}{a_1}, \quad \bar{\alpha} = \frac{\alpha_*}{\alpha}$$

As the units of length, time, velocity, pressure and temperature we use a_1 , a_1^2/ν_1 , ν_1/a_1 , $\rho_1 \nu_1^2/a_1^2$ and θ . The complete nonlinear equations governing convection are then written in the following dimensionless form:

$$\frac{\partial \mathbf{v}_m}{\partial t} + (\mathbf{v}_m \cdot \nabla) \mathbf{v}_m = -e_m \nabla p_m + c_m \Delta \mathbf{v}_m + b_m G T_m \mathbf{e} \tag{1}$$

$$\frac{\partial T_m}{\partial t} + \mathbf{v}_m \cdot \nabla T_m = \frac{d_m}{P} \Delta T_m \tag{2}$$

$$\nabla \mathbf{v}_m = 0, \quad m = 1, 2, 3 \tag{3}$$

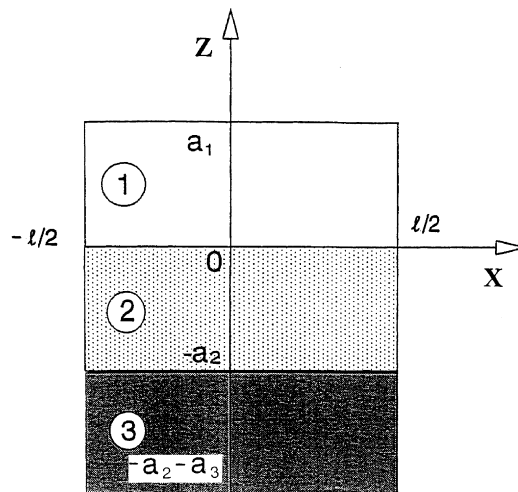


Fig. 1. Geometrical configuration of the three-layer system and coordinate axes.

where $e_1 = c_1 = b_1 = d_1 = 1$, $e_2 = \rho$, $c_2 = 1/\nu$, $b_2 = 1/\beta$, $d_2 = 1/\chi$, $e_3 = \rho_*$, $c_3 = 1/\nu_*$, $b_3 = 1/\beta_*$, $d_3 = 1/\chi_*$; $\Delta = \nabla^2$, $G = g\beta_1\theta a_1^3/\nu_1^2$ is the Grashof number, and $P = \nu_1/\chi_1$ is the Prandtl number, \mathbf{e} is the unit vector of the axis z .

The boundary conditions on the rigid boundaries are:

$$\mathbf{v}_1 = 0, \quad T_1 = 0 \quad \text{at } z = 1 \tag{4}$$

$$\mathbf{v}_3 = 0, \quad T_3 = 1 \quad \text{at } z = -a - a_* \tag{5}$$

We assume that the interfaces between fluids are flat and situated at $z = 0$ and $z = -a$, and put the following system of boundary conditions: at $z = 0$:

$$\frac{\partial v_{1x}}{\partial z} - \eta^{-1} \frac{\partial v_{2x}}{\partial z} - \frac{M}{P} \frac{\partial T_1}{\partial x} = 0, \quad \frac{\partial v_{1y}}{\partial z} - \eta^{-1} \frac{\partial v_{2y}}{\partial z} - \frac{M}{P} \frac{\partial T_1}{\partial y} = 0 \tag{6}$$

$$v_{1x} = v_{2x}, \quad v_{1y} = v_{2y}, \quad v_{1z} = v_{2z} = 0 \tag{7}$$

$$T_1 = T_2 \tag{8}$$

$$\frac{\partial T_1}{\partial z} - \kappa^{-1} \frac{\partial T_2}{\partial z} = 0 \tag{9}$$

at $z = -a$:

$$\eta^{-1} \frac{\partial v_{2x}}{\partial z} - \eta_*^{-1} \frac{\partial v_{3x}}{\partial z} - \frac{\bar{\alpha} M}{P} \frac{\partial T_3}{\partial x} = 0, \quad \eta^{-1} \frac{\partial v_{2y}}{\partial z} - \eta_*^{-1} \frac{\partial v_{3y}}{\partial z} - \frac{\bar{\alpha} M}{P} \frac{\partial T_3}{\partial y} = 0 \tag{10}$$

$$v_{2x} = v_{3x}, \quad v_{2y} = v_{3y}, \quad v_{2z} = v_{3z} = 0 \tag{11}$$

$$T_2 = T_3 \tag{12}$$

$$\kappa^{-1} \frac{\partial T_2}{\partial z} - \kappa_*^{-1} \frac{\partial T_3}{\partial z} = 0 \tag{13}$$

Here $M = \alpha\theta a_1/\eta_1\chi_1$ is the Marangoni number.

The boundary value problem given above has a solution:

$$\mathbf{v}_m = 0, \quad m = 1, 2, 3 \tag{14}$$

$$T_1 = T_1^0 = -\frac{(z-1)}{1 + \kappa a + \kappa_* a_*} \tag{15}$$

$$T_2 = T_2^0 = -\frac{(\kappa z - 1)}{1 + \kappa a + \kappa_* a_*} \tag{16}$$

$$T_3 = T_3^0 = -\frac{\kappa_* z - 1 + (\kappa_* - \kappa)a}{1 + \kappa a + \kappa_* a_*} \tag{17}$$

corresponding to the mechanical equilibrium.

3. Nonlinear approach

In the present Note, we simulate two-dimensional finite-amplitude flows in a finite region $-l/2 \leq x \leq l/2$, $-a_2 - a_3 \leq z \leq a_1$ (see Fig. 1). We introduce the stream function ψ_m and the vorticity ϕ_m ,

$$v_{m,x} = \frac{\partial \psi_m}{\partial z}, \quad v_{m,z} = -\frac{\partial \psi_m}{\partial x}$$

$$\phi_m = \frac{\partial v_{m,z}}{\partial x} - \frac{\partial v_{m,x}}{\partial z} \quad (m = 1, 2, 3)$$

and rewrite Eqs. (1) and (2) in the following form:

$$\frac{\partial \phi_m}{\partial t} + \frac{\partial \psi_m}{\partial z} \frac{\partial \phi_m}{\partial x} - \frac{\partial \psi_m}{\partial x} \frac{\partial \phi_m}{\partial z} = d_m \Delta \phi_m + b_m G \frac{\partial T_m}{\partial x} \tag{18}$$

$$\Delta \psi_m = -\phi_m \tag{19}$$

$$\frac{\partial T_m}{\partial t} + \frac{\partial \psi_m}{\partial z} \frac{\partial T_m}{\partial x} - \frac{\partial \psi_m}{\partial x} \frac{\partial T_m}{\partial z} = \frac{c_m}{P} \Delta T_m \quad (m = 1, 2, 3) \tag{20}$$

At the interfaces normal components of velocity vanish and the continuity conditions for tangential components of velocity, viscous stresses, temperatures, and heat fluxes also apply:

$$z = 0: \quad \psi_1 = \psi_2 = 0, \quad \frac{\partial \psi_1}{\partial z} = \frac{\partial \psi_2}{\partial z}, \quad T_1 = T_2 \quad (21)$$

$$\frac{\partial T_1}{\partial z} = \frac{1}{\kappa} \frac{\partial T_2}{\partial z}, \quad \frac{\partial^2 \psi_1}{\partial z^2} = \frac{1}{\eta} \frac{\partial^2 \psi_2}{\partial z^2} + \frac{M}{P} \frac{\partial T_1}{\partial x} \quad (22)$$

$$z = -a: \quad \psi_2 = \psi_3 = 0, \quad \frac{\partial \psi_2}{\partial z} = \frac{\partial \psi_3}{\partial z}, \quad T_2 = T_3 \quad (23)$$

$$\frac{1}{\kappa} \frac{\partial T_2}{\partial z} = \frac{1}{\kappa_*} \frac{\partial T_3}{\partial z}, \quad \frac{1}{\eta} \frac{\partial^2 \psi_2}{\partial z^2} = \frac{1}{\eta_*} \frac{\partial^2 \psi_3}{\partial z^2} + \frac{\bar{\alpha} M}{P} \frac{\partial T_2}{\partial x} \quad (24)$$

On the horizontal solid plates the boundary conditions read:

$$z = 1: \quad \psi_1 = \frac{\partial \psi_1}{\partial z} = 0, \quad T_1 = 0 \quad (25)$$

$$z = -a - a_*: \quad \psi_3 = \frac{\partial \psi_3}{\partial z} = 0, \quad T_3 = 1 \quad (26)$$

For simulations of cellular motions in an infinite layers, the periodic boundary conditions have been used on lateral walls $x = \pm L/2$, $L = l/a_1$:

$$\psi_m(x + L, z) = \psi_m(x, z); \quad \phi_m(x + L, z) = \phi_m(x, z); \quad T_m(x + L, z) = T_m(x, z) \quad (27)$$

The boundary value problem formulated above was solved by the finite-difference method. Eqs. (18)–(20) were approximated on a uniform mesh using a second-order approximation for the spatial coordinates. The nonlinear equations were solved using the explicit scheme, on a rectangular uniform mesh 56×112 . We checked the results on 56×168 and 112×168 meshes. The relative changes of the stream function amplitudes for all the mesh sizes do not exceed 2.5%. The time step was calculated by the formula

$$\Delta t = \frac{[\min(\Delta x, \Delta z)]^2 [\min(1, \nu, \chi, \nu_*, \chi_*)]}{2[2 + \max |\psi_m(x, z)|]}$$

where Δx , Δz are the mesh sizes for the corresponding coordinates. The Poisson equations were solved by the iterative Liebman successive over-relaxation method on each time step: the accuracy of the solution was 10^{-4} for the steady motion and 10^{-5} for the oscillations. The details of the numerical method can be found in the book by Simanovskii and Nepomnyashchy [1] (see also [8]).

4. Numerical results

Let us consider the system air–ethylene glycol–fluorinert FC75 (fluorocarbon-based fluid, perfluoro (2-butyl-tetrahydrofuran)) with the following set of parameters: $\nu = 0.974$, $\nu_* = 18.767$, $\eta = 0.001$, $\eta_* = 0.013$, $\kappa = 0.098$, $\kappa_* = 0.401$, $\chi = 215.098$, $\chi_* = 606.414$, $\beta = 2.62$, $\beta_* = 0.72$, $\bar{\alpha} = 0.080$. Fix the ratios of the layers thicknesses $a = a_* = 1$.

In the system under consideration, the flow of the thermocapillary origin takes place mainly near the upper interface, while the flow of the buoyancy origin is developed mainly in the bottom layer. Such an “indirect” interaction of both mechanisms of instability which is impossible in a system with a single interface, may lead to much more complex dynamics and unexpected effects.

The general diagram of nonlinear regimes is presented in Fig. 2. We shall start the discussion of the nonlinear results with the description of two types of stationary flows: (1) Marangoni flow weakly influenced by buoyancy (point A in Fig. 2) and (2) buoyancy flow weakly influenced by the thermocapillary effect (point B in Fig. 2). Streamlines and isolines of temperature deviations $T_m(x, z) - T_m^0(z)$ ($m = 1, 2, 3$; $T_m^0(z)$ is the equilibrium temperature field) for these flows are presented in Figs. 3 and 4, respectively. The flow of the thermocapillary origin takes place mainly near the upper interface (Fig. 3(a)), while the buoyancy convection is realized mainly in the bottom layer (Fig. 4(a)).

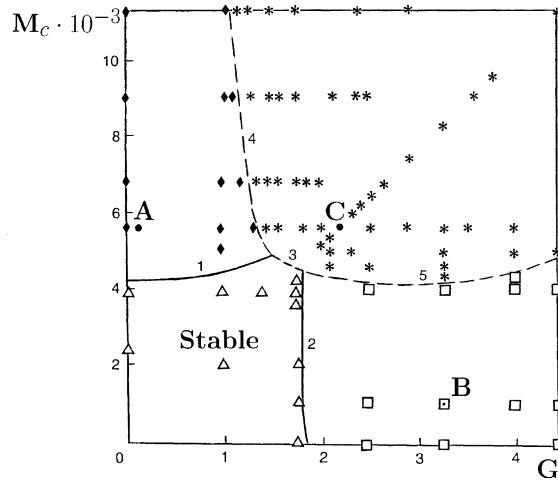


Fig. 2. The general diagram of flow regimes in the plane (M, G) ; Δ – equilibrium, \blacklozenge – steady flow (type I), \square – steady flow (type II), $*$ – traveling waves. Lines 1, 2 and 3 correspond to the boundaries of the linear stability theory; lines 4 and 5 separate the nonlinear steady flows and buoyant–thermocapillary traveling waves.

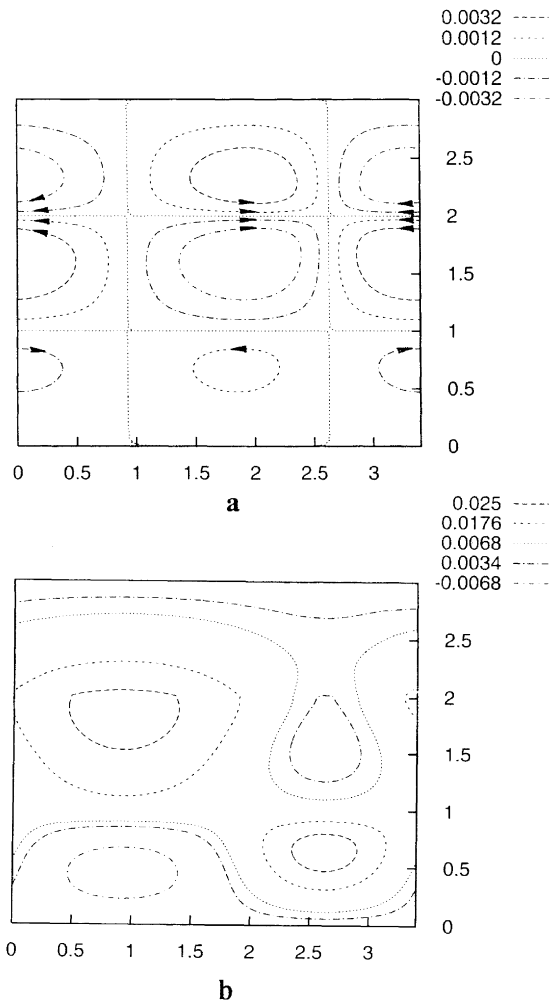


Fig. 3. (a) Stream lines and (b) isolines of temperature deviations for the steady flow (type I) at $M = 5700$, $G = 0.1$, $L = 3.4$.

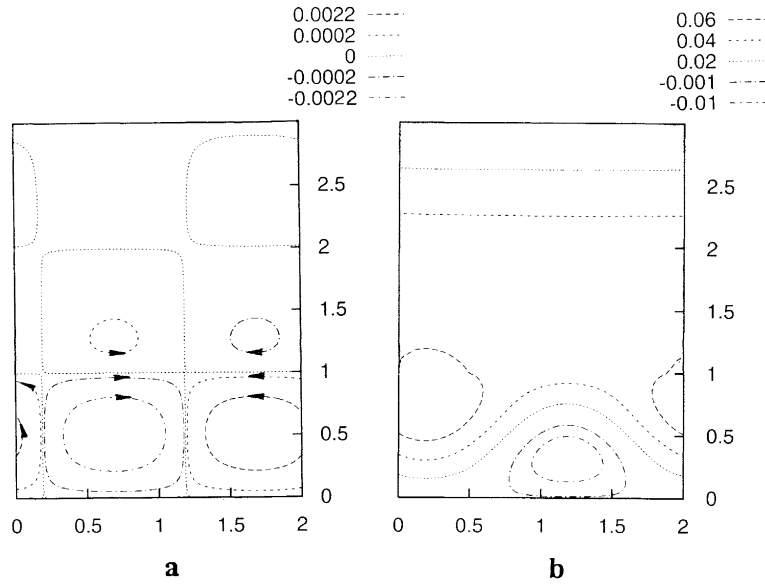


Fig. 4. (a) Stream lines and (b) isolines of temperature deviations for the steady flow (type II) at $M = 1000, G = 3.2, L = 2$.

Nonlinear results confirm the existence of the oscillatory flow: above the threshold predicted by the linear stability theory, the *nonlinear traveling wave* is developed

$$\psi_m(x, z, t) = \psi_m(x - ct, z), \quad T_m(x, z, t) = T_m(x - ct, z) \tag{28}$$

where c is the phase velocity of the traveling wave.

Snapshots of streamlines for the buoyant–thermocapillary traveling wave at different moments of time are presented in Fig. 5 (point C in Fig. 2). The traveling wave moves from the right to the left. The maximum values of stream functions in all the layers $\psi_{max,m} = \max \psi_m(x, z)$ ($m = 1, 2, 3$) are constant in time.

Under the conditions of the experiment, when the geometric configuration of the system is fixed while the temperature difference θ is changed, the Marangoni number M and the Grashof number G are proportional. We define the inverse dynamic Bond number

$$K = \frac{M}{GP} = \frac{\alpha}{g\beta_1\rho_1a_1^2}$$

Comparison of the maximum values of stream function in all the layers shows that the most intensive motion develops in the middle layer. With the increase of the Marangoni number, the period of the wave decreases, i.e., the phase velocity grows.

Let us use the following integral quantities, characterizing the intensity of motions in the left and in the right halves of the layers:

$$S_{l1}(t) = \int_{-L/2}^0 dx \int_0^1 dz \psi_1(x, z, t), \quad S_{r1}(t) = \int_0^{L/2} dx \int_0^1 dz \psi_1(x, z, t) \tag{29}$$

$$S_{l3}(t) = \int_{-L/2}^0 dx \int_{-a-a_*}^{-a} dz \psi_3(x, z, t), \quad S_{r3}(t) = \int_0^{L/2} dx \int_{-a-a_*}^{-a} dz \psi_3(x, z, t) \tag{30}$$

The time evolution of the quantities $S_{lm}(t)$, $m = 1, 2, 3$, shows that oscillations keep rather simple almost sinusoidal form. Even on a large distance from the linear stability boundary (see line 3 in Fig. 2; $M \leq 228\,000$) the oscillatory flow keeps its periodicity for the fixed value of K ($K = 3682$). The phase trajectory presented in Fig. 6 demonstrates a significant phase delay of the oscillations in the top layer with respect to the oscillations in the bottom layer. For

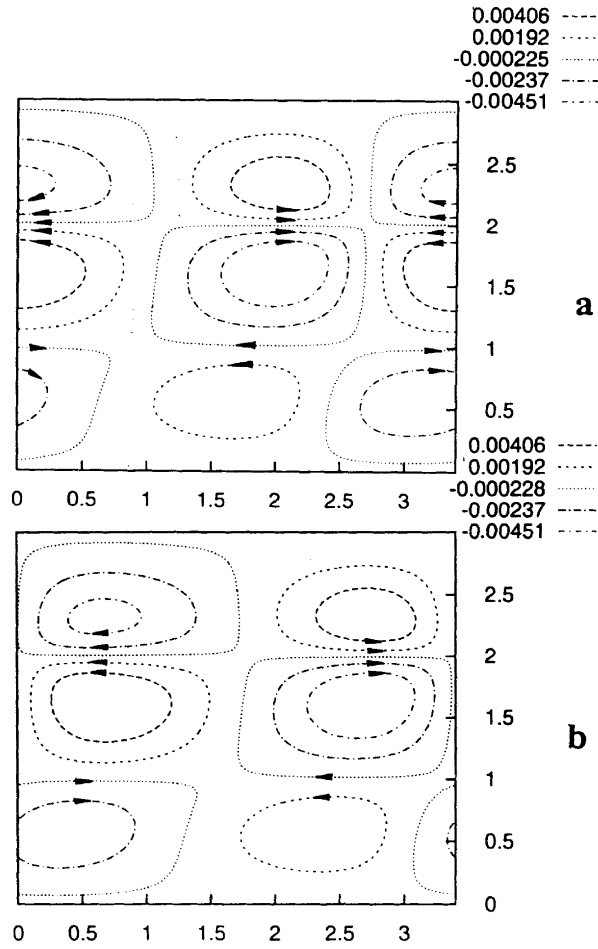


Fig. 5. (a), (b) Snapshots of stream lines for a buoyant-thermocapillary traveling wave at $M = 5700$, $G = 2.15$, $L = 3.4$.

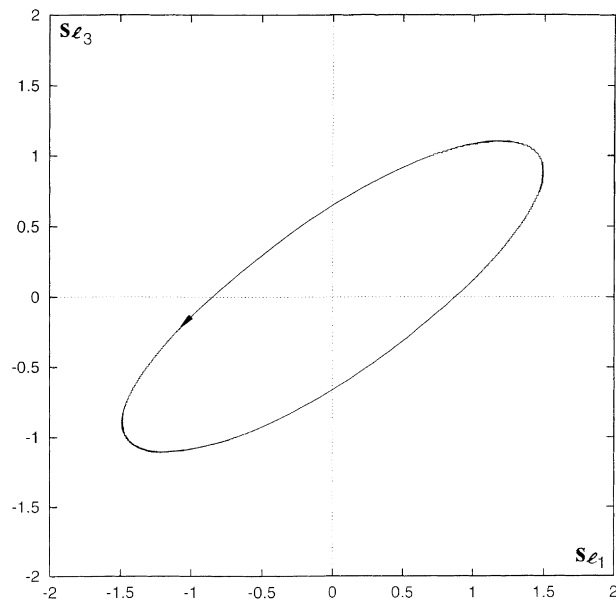


Fig. 6. Phase trajectory $S_{l3}(S_{l1})$ for the oscillatory flow at $M = 5700$, $G = 2.15$, $L = 3.4$.

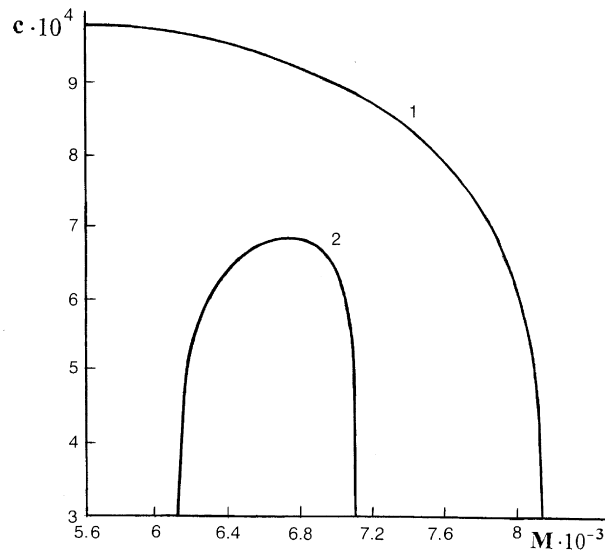


Fig. 7. Dependence of the wave velocity c on the Marangoni number M for the modulated traveling waves; $K = 1944$ (line 1); $K = 1495$ (line 2); $L = 3.4$.

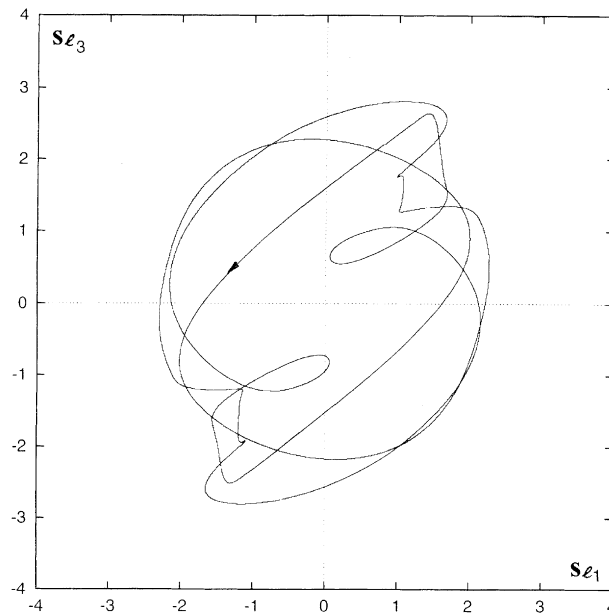


Fig. 8. Phase trajectory $S_3(S_1)$ for the modulated traveling wave at $M = 6140$, $K = 1495$, $L = 3.4$.

this motion, the thermocapillary convection in the top and middle layers coexists with the buoyancy convection in the bottom layer.

Let us discuss now the evolution of flow regimes by changing the inverse dynamic Bond number. The decrease of K (the weakening of the thermocapillary effect) leads to the appearance of a new convective regime: the buoyant–thermocapillary wave is destabilized, and the *modulated traveling wave* is developed in the system. The maximum values of stream function ($\psi_{max,m}$) ($m = 1, 2, 3$) are not constant in time any more and oscillate in a periodic way. The dependence of the phase velocities on the Marangoni number for different values of the inverse dynamic Bond number K , are shown in Fig. 7. One can see that for $K = 1495$ (line 2 in Fig. 7), the phase velocity changes in a non-monotonic way. The multi-loop phase trajectory, corresponding to the modulated traveling wave, is presented in Fig. 8.

5. Conclusion

The nonlinear regimes of convection in a multilayer system are investigated. The periodic boundary conditions on the lateral boundaries, are considered. It is shown that the joint action of buoyancy and thermocapillary effect, leads to the development of nonlinear traveling wave. For this flow, the thermocapillary convection in the top and middle layers coexists with the buoyancy convection in the bottom layer. The oscillatory flow keeps its periodicity even on a large distance from the linear stability boundary. The phase diagram on the plane the Grashof number–the Marangoni number is constructed. The weakening of the thermocapillary effect leads to the development of the modulated traveling wave in the system. For this flow, the maximum values of the stream function in all the layers oscillate in a periodic way.

References

- [1] I.B. Simanovskii, A.A. Nepomnyashchy, *Convective Instabilities in Systems with Interface*, Gordon and Breach, London, 1993.
- [2] A. Nepomnyashchy, I. Simanovskii, J.-C. Legros, *Interfacial Convection in Multilayer Systems*, Springer, New York, 2006.
- [3] G.Z. Gershuni, E.M. Zhukhovitsky, *Convective Stability of Incompressible Fluid*, Keter, Jerusalem, 1976.
- [4] J.R.A. Pearson, On convection cells induced by surface tension, *J. Fluid Mech.* 4 (1958) 489.
- [5] A.A. Nepomnyashchy, I.B. Simanovskii, Thermocapillary and thermogravitational convection in a two-layer system with a distorted interface, *Fluid Dyn.* 19 (1984) 494.
- [6] A. Juel, J.M. Burgess, W.D. McCormick, J.B. Swift, H.L. Swinney, Surface-tension-driven convection patterns in two liquid layers, *Physica D* 143 (2000) 169.
- [7] A.A. Nepomnyashchy, I.B. Simanovskii, L.M. Braverman, Convective oscillations in multilayer systems under the combined action of buoyancy and thermocapillary effect, *Phys. Fluids* 17 (2005) 022103.
- [8] A.A. Nepomnyashchy, I.B. Simanovskii, Combined action of different mechanisms of instability in multilayer systems, *Phys. Rev. E* 59 (1999) 6672.